INTERNATIONAL JOURNAL OF CLIMATOLOGY
Int. J. Climatol. **31**: 847–862 (2011)
Published online 25 March 2010 in Wiley Online Library
(wileyonlinelibrary.com) DOI: 10.1002/joc.2129

RMetS
Royal Meteorological Society

Interannual variations of early summer monsoon rainfall over South China under different PDO backgrounds

Jiangyu Mao,[a]* Johnny C. L. Chan[b] and Guoxiong Wu[a]

[a] *State Key Laboratory of Numerical Modeling for Atmospheric Sciences and Geophysical Fluid Dynamics (LASG), Institute of Atmospheric Physics, Chinese Academy of Sciences, Beijing, China*

[b] *Laboratory for Atmospheric Research, Department of Physics and Materials Science, City University of Hong Kong, Hong Kong, China*

ABSTRACT: The interannual variations of the early summer South China monsoon rainfall (SCMR) in relation to different Pacific Decadal Oscillation (PDO) backgrounds are examined using station rainfall data and the European Centre for Medium-range Weather Forecasts (ECMWF) 40-year reanalysis (ERA-40) data. The objective of this study is to investigate the atmospheric circulation patterns responsible for such variations, thereby understanding the interdecadal modulation and the cause for the extreme wet and dry SCMR.

The interannual SCMR variance shows an interdecadal change before and after the late 1970s, with significant differences in sea-surface temperature (SST) and atmospheric circulation anomalies between the negative (1958–1976) and positive (1980–1998) PDO epochs. The dominant atmospheric teleconnection patterns associated with extreme wet and dry SCMR are remarkably different in these two epochs. During 1958–1976, an anomalous wet (dry) SCMR is characterized by a significantly anomalous anticyclone (cyclone) over the South China Sea (SCS) and western Pacific in the lower troposphere in the form of a meridional wave-like coupling along the coast of western North Pacific in the early summer, and preceded by a monopole circulation anomaly over the Ural Mountain in the preceding winter. During 1980–1998, however, an anomalous wet (dry) SCMR features a relatively weak anomalous anticyclone (cyclone) over the SCS in the low level without a significantly meridional juxtaposition of anomalous circulations in the early summer, and it follows a remarkable coherent long wave train pattern in middle-high latitudes in the preceding winter. Such interdecadal differences in anomalous circulation structures suggest that the relative roles of internal atmospheric variability and external forcing may be different from different epochs. But for both epochs, the circulation anomaly over the Ural Mountain shows a highly negative correlation with anomalous SCMR, suggesting that the winter circulation anomaly around the Ural Mountain is of great significance for improving the seasonal prediction of SCMR. Copyright © 2010 Royal Meteorological Society

KEY WORDS early summer monsoon rainfall; interannual variation; Pacific Decadal Oscillation (PDO); teleconnection

Received 17 February 2009; Revised 9 December 2009; Accepted 16 February 2010

1. Introduction

The empirical relationship between the Indian summer monsoon and El Niño/Southern Oscillation (ENSO) has been recognized extensively, in which a deficient (abundant) Indian monsoon rainfall is generally associated with a warm (cold) event in the eastern equatorial Pacific (e.g. Shukla and Paolino, 1983; Webster and Yang, 1992; Webster *et al*., 1998). However, such an inverse relationship has remarkably weakened since the late 1970s (e.g. Kumar *et al*., 1999; Torrence and Webster, 1999; Chang *et al*., 2001). Kumar *et al*. (1999) related this breakdown to a southeastward shift in the Walker circulation anomalies associated with ENSO and a change in land–ocean thermal contrast due to increased surface temperature over Eurasia in winter and spring. Chang *et al*. (2001) showed that another likely cause for the broken relationship is the strengthening and poleward shift of the jet stream over the North Atlantic, with the latter enhancing the European surface temperature anomalies in winter and spring. The effect of the resulting meridional temperature contrast disrupts the influence of ENSO on the Indian monsoon. Actually, the timing of this change in the relationship between ENSO and the Indian monsoon rainfall coincides with the interdecadal change in the Pacific sea-surface temperature (SST, e.g. Graham, 1994; Zhang *et al*., 1997) and the El Niño properties (Wang, 1995) as well as with climate changes in the Northern Hemisphere (Trenberth, 1990; Graham *et al*., 1994). Krishnamurthy and Goswami (2000) suggested that the interdecadal variations of the Indian summer monsoon are strongly correlated with those of various ENSO indices. Krishna and Sugi (2003) reported that the Indian monsoon is more vulnerable to drought situations, when El Niño events occur during warm phases of the Pacific interdecadal variability. Conversely, wet monsoons are more likely to prevail, when La Niña events coincide during cold phases

* Correspondence to: Jiangyu Mao, State Key Laboratory of Numerical Modeling for Atmospheric Sciences and Geophysical Fluid Dynamics (LASG), Institute of Atmospheric Physics, Chinese Academy of Sciences, P.O. Box 9804, Beijing 100029, China.
E-mail: mjy@lasg.iap.ac.cn

of the Pacific interdecadal variability. The Pacific SST interdecadal variability could thus be one more important player in affecting the interannual monsoon variability.

As an important component of the Asian monsoon system, the interannual variability of the East Asian monsoon is also modulated by the interdecadal fluctuations in the Pacific SST anomalies (Ding, 2007). Wu and Wang (2002) compared the East Asian summer monsoon–ENSO relationship before and after the late 1970s, and found significant changes in the location and intensity of anomalous convection over the western North Pacific and India. After the late 1970s, the convection anomaly over the western North Pacific enhanced and shifted to high latitudes due to increased summer mean SST in the Philippine Sea, which induced an eastward shift of an anomalous low pressure from East Asia to the North Pacific along 30°–45°N during the decaying phases of El Niño. Thus, anomalous winds over northeastern China and Korea switched from southeasterly to northeasterly. Before the late 1970s, an anomalous barotropic anticyclone developed over East Asia and anomalous southerlies prevailed over northeastern China during decaying phases of El Niño. This may be related to anomalous Indian convection through a zonal wave pattern along 30°–50°N. After the late 1970s, anomalous Indian convection weakened, which reduced the impact of the Indian convection on the East Asian summer monsoon. In investigating the associations of the summer (May–August) rainfall over the Yangtze Basin and/or pre-monsoon (May–June) rainfall over South China with the tropical SST anomalies, Chang *et al*. (2000a, 2000b) argued that the relationships between the East Asian summer monsoon and the eastern Pacific SST anomalies on both interannual and interdecadal timescales are mostly due to the variations of the western North Pacific subtropical anticyclone.

With the northward seasonal march of the East Asian summer monsoon, heavy rainfall first occurs over South China in early to mid-May, and early summer (May–June) is thus the main rainy season there (Ding, 1994, 2007). Both Chan and Zhou (2005) and Zhou *et al*. (2006) used rainfall observations at three stations (Hong Kong, Macao and Guangzhou) to construct an index for representing the early summer South China monsoon rainfall (SCMR), and found that its temporal variations exhibit a significant interdecadal oscillation. They suggested that such an interdecadal mode is related to the Pacific Decadal Oscillation (PDO) (e.g. Mantua *et al*., 1997) and ENSO. For example, when ENSO and PDO are in phase, i.e. high PDO phase/El Niño events or low PDO phase/La Niña events, SCMR tends to be below or above normal more often respectively. But in an out-of-phase ENSO–PDO relationship, the number of years with below and above-normal SCMR is similar, which suggests that the ENSO and PDO forcing of SCMR apparently cancel each other; thus, the inherent and unpredictable internal atmospheric variability (e.g. Palmer and Anderson, 1994; Lau, 1997) is likely be dominant.

Since the ENSO teleconnections with SCMR depend on the phases of the PDO, the interannual SCMR behaviour may also be different in different interdecadal epochs. The objective of this study is therefore to investigate the atmospheric circulation patterns related to interannual SCMR variations under different PDO regimes, thereby understanding the cause for the extreme wet and dry SCMR. Section 2 describes the data used in this paper. Section 3 compares interdecadal anomalies between two PDO epochs. Section 4 addresses interannual SCMR variations relative to different PDO backgrounds. Section 5 gives conclusions and discussions.

2. Data and methods

Monthly rainfall data from three stations, Hong Kong, Macao and Guangzhou, used in present study are the same as those in Chan and Zhou (2005), and they are available since 1910 and obtained from the respective weather bureaus. The SCMR index is defined as the bimonthly (May–June) rainfall average of these three stations for each individual year.

The PDO index derived from the leading principal component of the North Pacific monthly SST (poleward of 20°N) variability (Mantua *et al*., 1997) is taken from the website (http://jisao.washington.edu/pdo) and is available since 1900. Monthly SST data from 1957 to 2002 are extracted from the UK Met Office Hadley Centre's Sea Ice and SST data sets (HadISST1). The HadISST1 replaces the Global Sea Ice and Sea Surface Temperature (GISST) data sets, and is a unique combination of monthly globally complete fields of SST and sea ice concentration on a $1^\circ \times 1^\circ$ latitude–longitude grid from 1870 to date (Rayner *et al*., 2003). Monthly mean sea level pressure (SLP) data are also the products (HadSLP2) of Met Office Hadley Centre, which are recently created by blending together the processed terrestrial and marine pressure observations with a $5^\circ \times 5^\circ$ resolution since 1850 (Allan and Ansell, 2006). Monthly atmospheric circulation data for the period September 1958–August 2002 are obtained from the European Centre for Medium-range Weather Forecasts (ECMWF) 40-year reanalysis (ERA-40) products to demonstrate the anomalous circulation patterns associated with the recent positive and negative phases of the interdecadal oscillations.

According to the evolution of PDO index (Mantua *et al*., 1997), there are two predominantly positive PDO epochs (1925–1946, after 1977) and one negative epoch (1947–1976). However, available ERA-40 circulation data only overlap the two most recent epochs. Thus, to reveal the interdecadal change in the late 1970s, the negative epoch (1958–1976) and the positive (1980–1998) epoch are selected, with each epoch comprising 19 years. To clarify signatures of the influence of different PDO backgrounds on the interannual SCMR variations, some transition years such as 1977–1979 and after 1999 are excluded.

To validate the classification of the two epochs based on the PDO index, Figure 1 displays the time series of

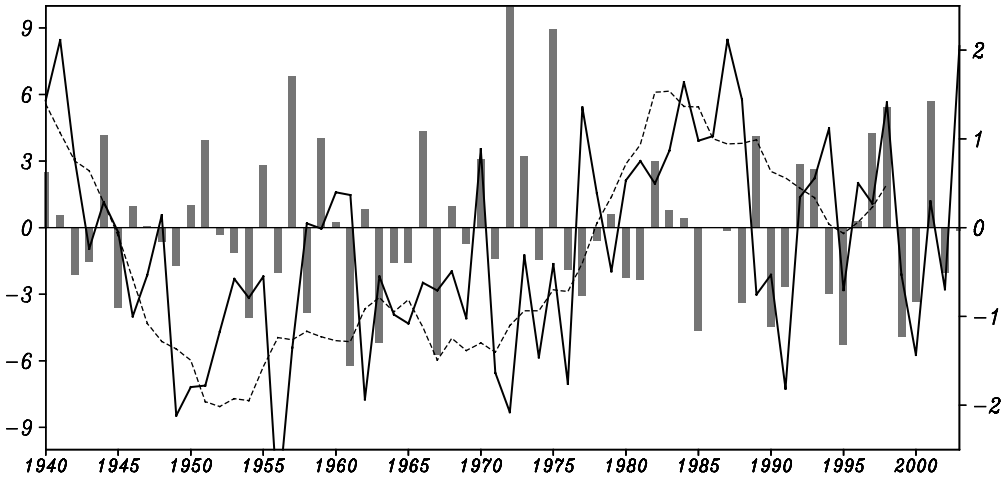

Figure 1. Time series of SCMR anomaly (bar, mm day^{-1}, with scale on the left-hand ordinate) and standardized wintertime (November–March) PDO index (solid line) and its 11-year running mean (dashed line, with scale on the right-hand ordinate). The SCMR anomaly is calculated as departure from the long-term mean of 10.8 mm day^{-1} for the base period 1940–2003. The interannual standard deviation of SCMR anomaly for this period is 3.5 mm day^{-1}.

SCMR anomaly and wintertime PDO index during the period 1940–2003. The long-term mean of SCMR for this period is 10.8 mm day^{-1}, with the standard deviation of interannual variations being 3.5 mm day^{-1}. A 11-year running mean of the PDO index clearly shows a negative PDO phase between 1946 and 1976 and a positive PDO phase after 1980. Transition years from positive to negative phases or vice versa occurred around 1945 and 1978, but actual shifts may not be exactly in these two years. From Figure 1, one can note that the recent positive PDO epoch appears to decay since the late 1980s, with the positive behaviour in the period 1989–1998 being less dominant than in the period 1980–1988 due to three consecutive negative PDO indices appearing from 1989 to 1991 as well as negative PDO indices in 1994 and 1995. Thus, some studies have argued that a regime shift possibly occurred in the winter of 1988/89 (e.g. Overland *et al*., 1999; Hare and Mantua, 2000). However, others have suggested that the recent positive PDO regime persists through (at least) 1997 (e.g. Mantua *et al*., 1997; McGowan *et al*., 1998). Therefore, the existence of the 1989 regime shift remains controversial and needs to be further studied. Here, our present result accords with the latter of the above studies. The 11-year running mean PDO index (Figure 1) is noted to remain positive till 1998 in which the PDO data prior to 2003 has been included, indicating that the period 1989–1998 belongs to the same PDO epoch as the period 1980–1988. To further verify our classification, we have calculated interdecadal differences of SLP fields between the periods 1980–1988 and 1989–1998, similar to Figure 3 (as shown below). Because SLP changes are closely linked to changes in surface winds, and thereby to changes in SST (Wang *et al*., 2000), the SLP field is used to demonstrate whether the statistically significant differences exist before and after 1989 in terms of atmospheric circulations. Results show that there are scarcely any areas especially in the North Pacific where the differences between the mean values of the two periods are statistically significant from zero even at the 90% confidence level (based on Student's *t*-test), indicating that for atmospheric circulations there are no statistically significant differences between these two periods. Therefore, in the present study, we consider the entire period 1980–1998 as a positive PDO phase, although it is not possible to infer with great confidence how long this phase persists and in which year the PDO changes into the negative phase. The periods 1958–1976 and 1980–1998 are thus selected to represent negative and positive PDO epochs for a comparison with the same number of years within each epoch and with the least amount of ambiguity.

3. Interdecadal anomalies during the two PDO phases

Before discussing the interannual variability of SCMR in different PDO epochs, we should examine the interdecadal differences between the negative and positive PDO phases. Figure 2 shows the composite seasonal evolutions of SST anomalies for negative and positive PDO categories. For the negative PDO phase (Figure 2(a)–(c)), significant positive SST anomalies are found in the midlatitude North Pacific, while negative SST anomalies are present in the eastern Pacific, with significant anomalies on both sides of the equator. The SST anomaly distributions in the Pacific exhibit the typical features of the negative PDO phase (e.g. Mantua *et al*., 1997). Note that negative SST anomalies are also observed over the Indian Ocean. The entire pattern in the Pacific and Indian Oceans displays some features similar to a La Niña event, and it persists unusually from the preceding winter months to early summer. Thus, PDO and ENSO appear to be related (e.g. Zhang *et al*., 1997). Of course, insignificant SST anomalies in the eastern equatorial Pacific are different from a typical model of a La Niña event, which results from the counteraction between

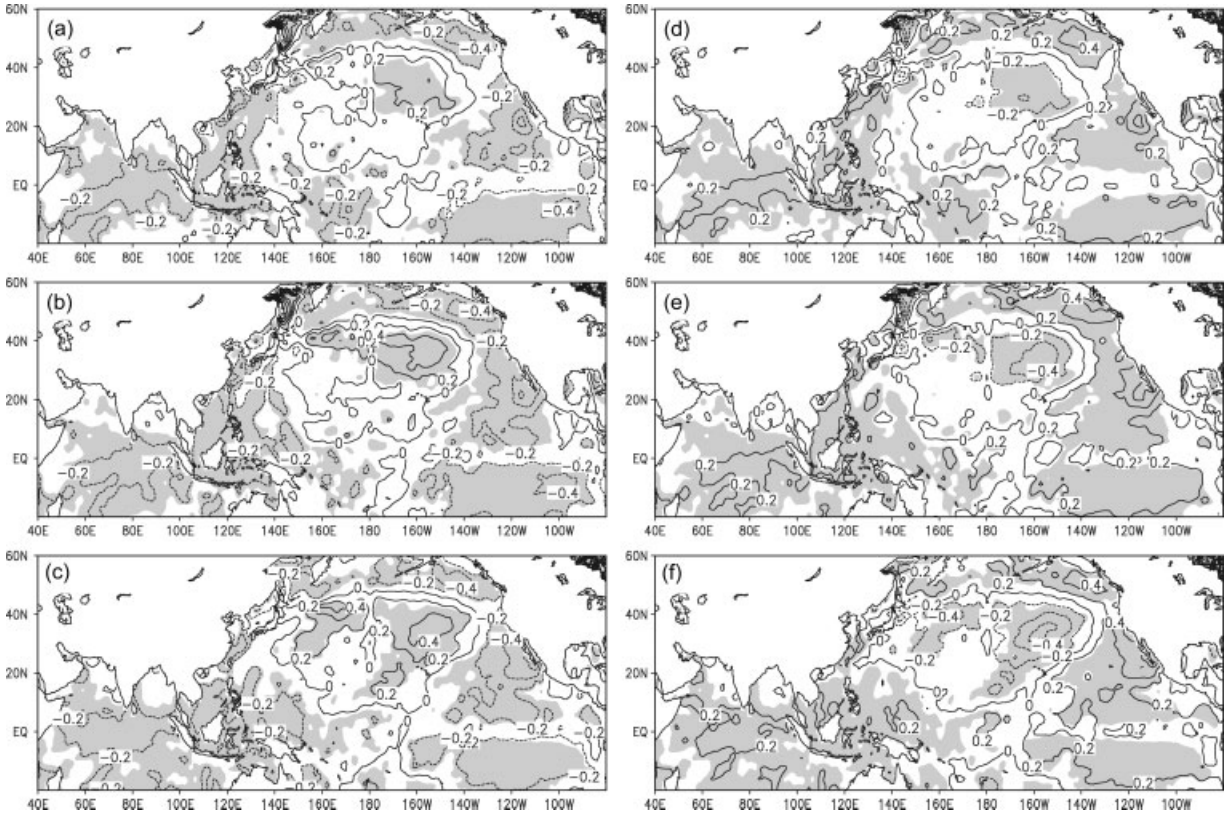

Figure 2. Composite bimonthly patterns of SST anomalies (K) for negative PDO (1958–1976, left panels) and positive PDO (1980–1998, right panels) phases in the months January–February, March–April and May–June from (a) to (c) and from (d) to (f). Anomalies are calculated as departures from the 1958–2002 base period means. Shading denotes regions of the *t*-test significance at the 95% confidence level.

El Niño events and La Niña events within this epoch. In contrast, during the positive PDO phase, unusually persistent SST anomalies of an El Niño-like pattern are prominent from the preceding winter to early summer (Figure 2(d)–(f)), implying that El Niño events predominate over La Niña events during the period 1980–1998. Whether PDO and ENSO are independent of each other or not, such two different SST anomaly patterns likely exert different modulating effects on the ENSO teleconnections during the two epochs. As emphasized by Namias *et al.* (1988), persistent SST anomaly patterns in the North Pacific are often associated with persistent atmospheric teleconnection patterns. Different SST anomaly patterns in the entire Pacific and Indian Oceans in two epochs can thus induce different dominant atmospheric teleconnection patterns.

Composite seasonal evolutions of SLP anomalies demonstrate that in the negative PDO phase, the atmospheric response is mainly characterized by negative SLP anomalies over the western and central Pacific from 0° to 20°N and positive anomalies over the eastern Aleutian Basin, roughly forming a dipole anomaly pattern in the Pacific (Figure 3(a) and (b)). Gershunov and Barnett (1998) suggested that in winter the atmospheric pressure anomaly in the Aleutian region is sensitive to the ENSO phase. Latif and Barnett (1996) and Barnett *et al.* (1999) conducted sensitivity experiments with the coupled ocean-atmospheric general circulation model and demonstrated that positive SST anomalies in the midlatitude North Pacific induce a weakened Aleutian low. Thus, the positive anomalies over the Aleutian Basin may indicate a typical response of the negative PDO–La Niña combination. As the season evolves, the negative anomaly region in tropical Pacific extends northeastward, while the positive anomaly area in the Aleutian Basin shrinks. Also observed are positive SLP anomalies over northern China and Mongolia, accompanied by negative anomalies to the south. By early summer (Figure 3(c)), the negative anomalies prevail over most of China and South Asia. Conversely, during the positive PDO phase (Figure 3(d)–(f)), persistent positive SLP anomalies exist over tropical western and central Pacific, with negative anomalies over the Aleutian Basin. Latif and Barnett (1996) suggested that this interdecadal variability originates from an unstable ocean–atmosphere interaction over the North Pacific. It is noteworthy that in the early summer season, negative SLP anomalies cover almost the entire Asian continent during 1958–1976, but positive anomalies are found during 1980–1998, which indicates that positive SCMR anomalies are more likely to occur during the former than during the latter.

The interdecadal differences in the middle troposphere can be found from composite anomalies of the 500-hPa streamfunction. During the negative PDO phase, a pair of zonally stretched anomalous anticyclonic circulations is observed over the midlatitudes, one covering the Eurasia continent and the other covering the midlatitude North Pacific, while an anomalous cyclonic circulation

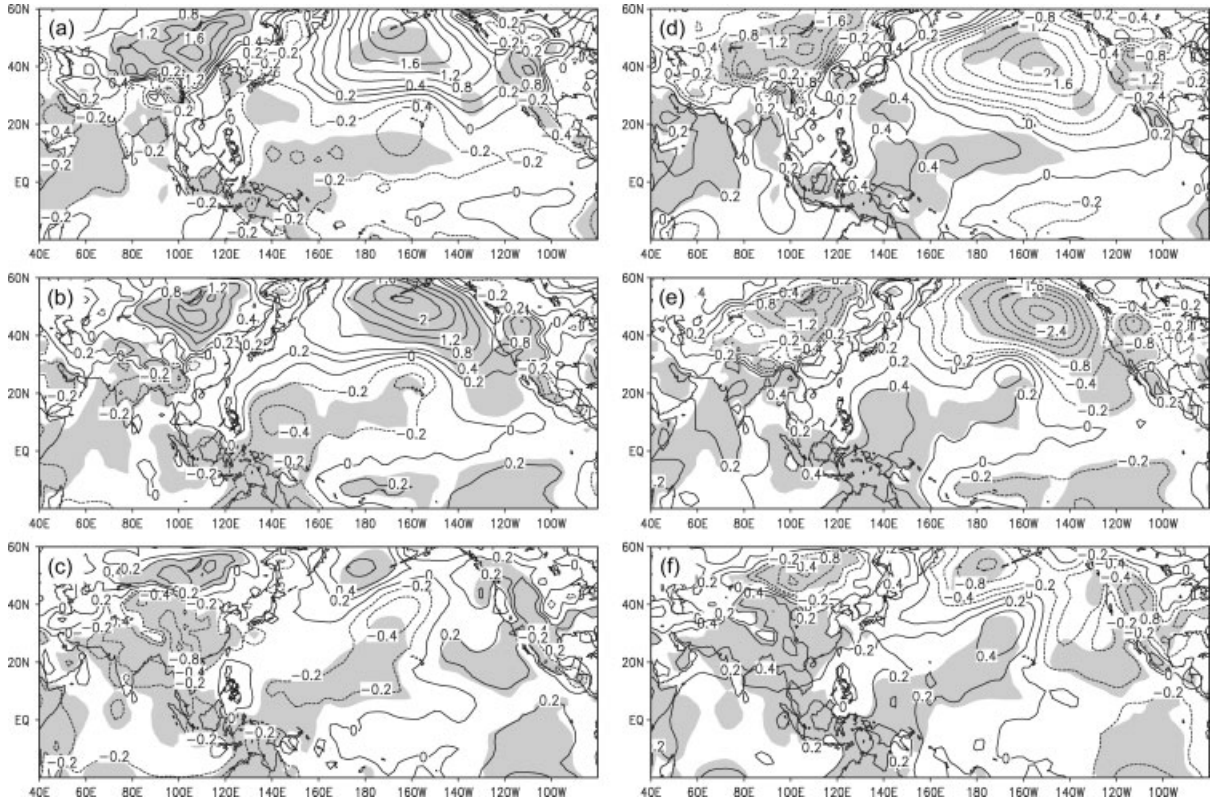

Figure 3. As in Figure 2 except for SLP anomalies (hPa).

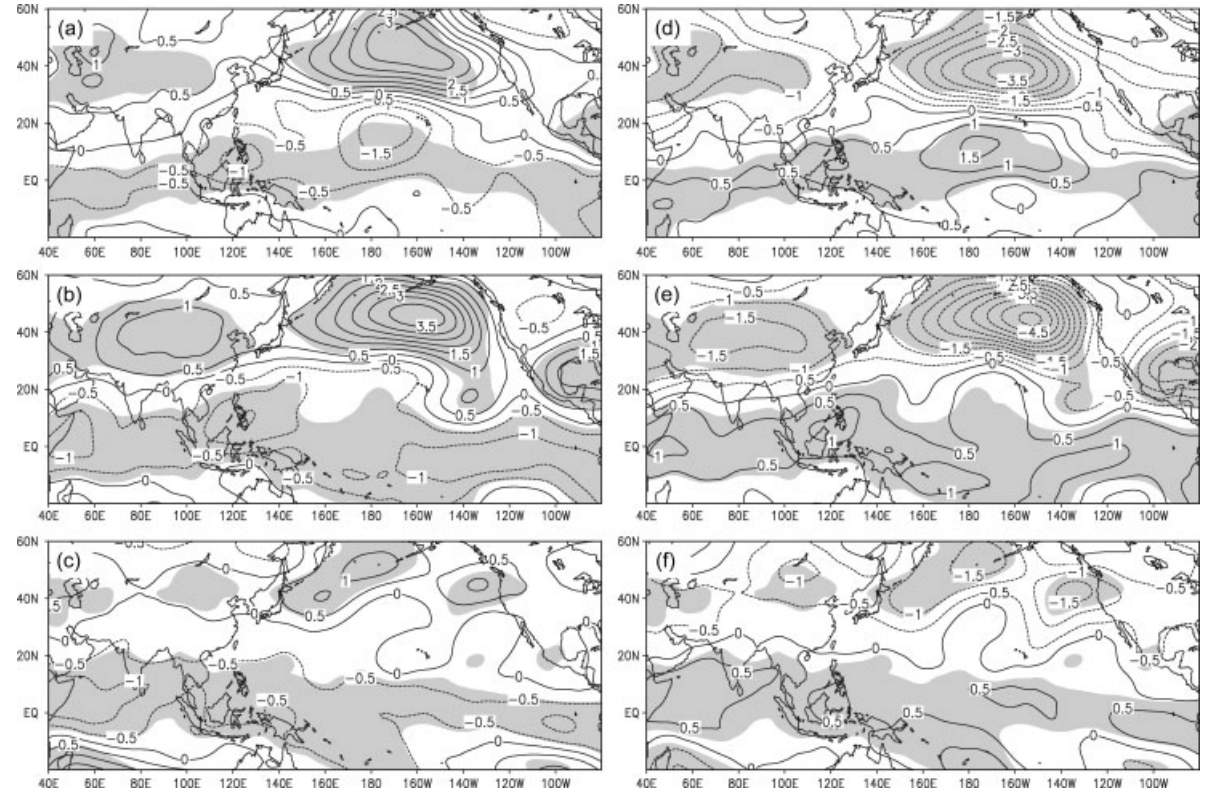

Figure 4. As in Figure 2 except for 500-hPa streamfunction anomalies (10^6 m^2 s^{-1}).

prevails over the Tropics (Figure 4(a) and (b)). The mid-latitude positive anomalies indicate that for the period 1958–1976, the high-pressure ridges in front of and behind the East Asian low-pressure trough are stronger than normal in winter and spring. But in early summer (Figure 4(c)), such positive anomalies weaken. The

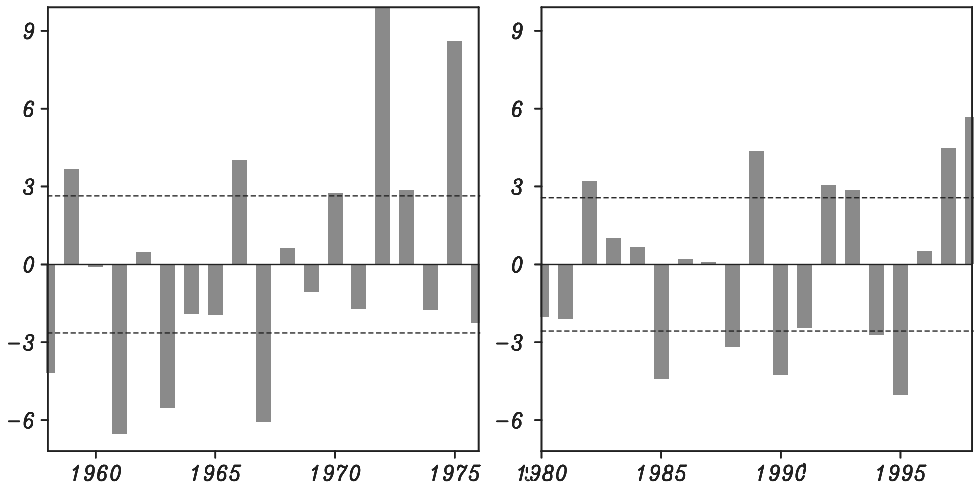

Figure 5. Time series of SCMR anomaly (bar, mm day^{-1}) for two epochs 1958–1976 and 1980–1998. Parallel dashed lines for the period 1958–1976 represent 0.6σ (σ is standard deviation of 4.4 mm day^{-1}), while for the period 1980–1998 they represent 0.8σ (σ is standard deviation of 3.2 mm day^{-1}). The thresholds of the actual SCMR anomalies indicated by parallel dashed lines in both epochs are identical.

negative anomalies suggest a below-normal tropical pressure system, roughly corresponding to the negative SLP anomalies (Figure 3(a)–(c)). The opposite flow patterns occur in the positive PDO phase (Figure 4(d) and (e)), with negative streamfunction anomalies over the midlatitudes and with positive anomalies in the Tropics. The negative anomalies over Eurasia continent indicate an anomalous cyclonic circulation with a weakened westerly jet stream. Chang *et al*. (2001) considered such flow patterns as a noted feature of the positive phase of the North Atlantic oscillation (NAO; Hurrell, 1995), and argued that the stronger influence of the Eurasia surface temperature on the interannual variation of the Indian monsoon in the most recent decades may be caused by the strengthening positive phase of the NAO and the associated jet stream patterns over the North Atlantic and northern Eurasia. The negative anomalies in the Tropics in Figure 4(c) indicate that the subtropical anticyclone is weaker during 1958–1976 than during 1980–1998, while the Asian monsoon trough is stronger during the former than during the latter. The opposite circulation anomalies over Eurasian continent imply that cold air activities tend to be stronger during 1958–1976 than during 1980–1998. Thus, positive SCMR anomalies are more likely to occur in the former than in the latter. Note that there are two extreme wet SCMR occurring in 1972 and 1975, and both belong to the period 1958–1976. It is obvious that these inerdecadal circulation anomalies exert an influence on the interannual variability of SCMR mainly through modulating the atmospheric circulation in the Tropics and midlatitudes.

Similar features are observed in the upper troposphere from the corresponding 200-hPa geopotential height anomaly patterns (not shown). During 1958–1976, positive height anomalies centred over northwestern China and North Pacific are accompanied by negative height anomalies to the south, in a band that covers most of the Tropics south of 20°N. The opposite situations occur during 1980–1998. A comparison of Figures 3 and 4 together with the 200-hPa height anomaly patterns indicates that interdecadal anomalous signals from lower to upper troposphere during the negative and positive PDO phases exhibit a pronounced barotropic structure.

4. Interannual SCMR variations relative to different PDO backgrounds

4.1. Spatial structures

The above analyses show that significant differences exist between the negative and positive PDO phases in terms of anomalous SSTs and atmospheric circulations. During each PDO phase, this interdecadal anomalous circulation as a background would certainly modify the intensity and location of subtropical anticyclone and related Asian monsoon trough as well as the midlatitude circulation over the Eurasian continent. Thus, the anomalous atmospheric circulation patterns responsible for the interannual variability of SCMR are examined relative to these two different PDO regimes. We now compare the spatial circulation structures associated with anomalous wet and dry SCMR. The time series of SCMR anomaly from 1958 to 1976 and from 1980 to1998 are separately shown in Figure 5. The mean value of 11.1 mm day^{-1} for the period 1958–1976 is slightly different from that of 10.6 mm day^{-1} for the period 1980–1998, but this difference is not significant at the 95% confidence level based on the t-test. However, the variance of the interannual SCMR variations is larger during 1958–1976 than during 1980–1998, with different standard deviations of 4.4 and 3.2 mm day^{-1}, respectively. Based on the F-test, the shift in the variance is statistically significant at the 95% confidence level, reflecting the interdecadal change of SCMR.

To investigate the interannual variability of SCMR under different PDO backgrounds, anomalous wet and dry SCMR years should be classified based on an objective criterion for these two epochs. In Figure 5,

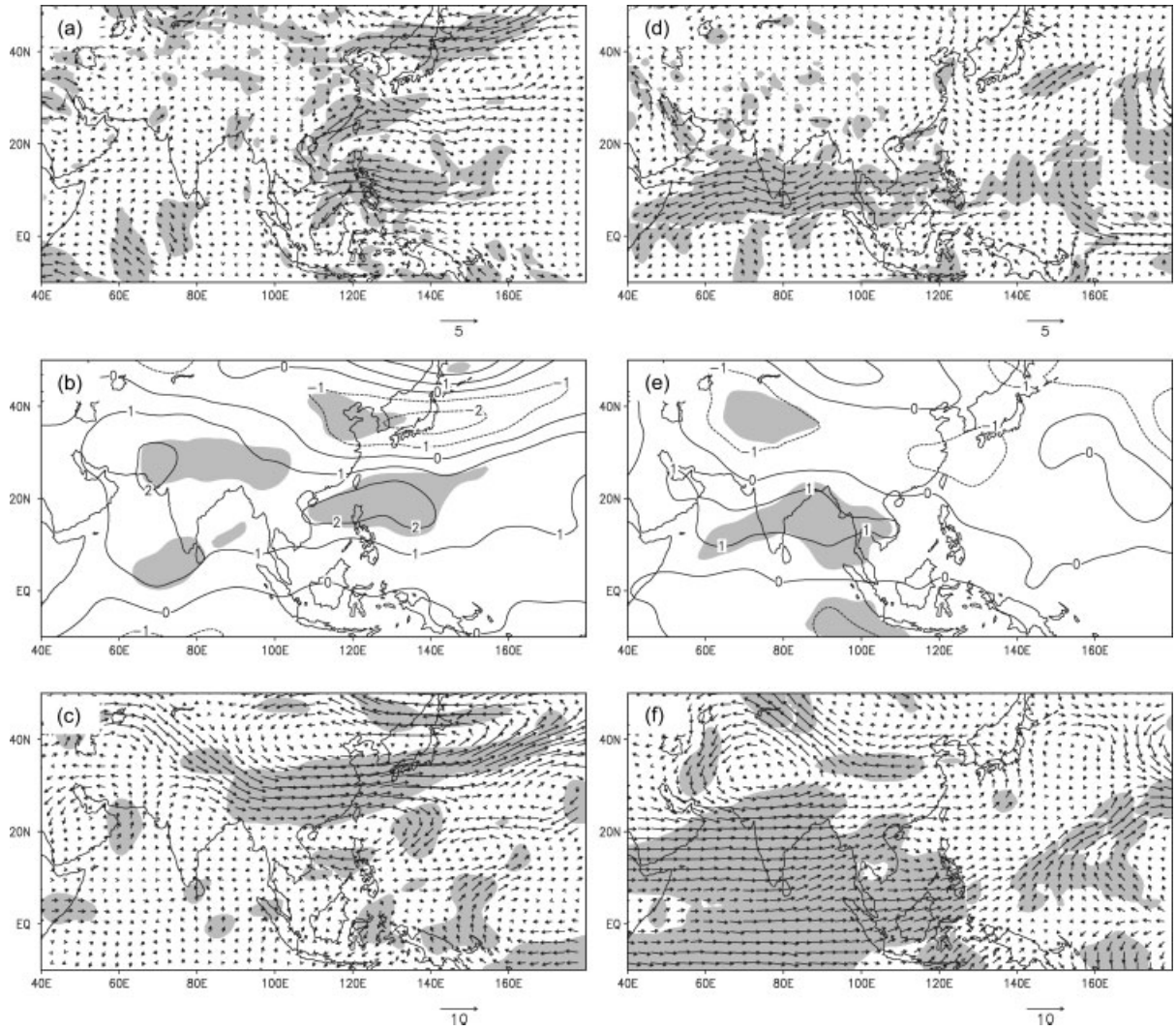

Figure 6. Composite wet-minus-dry bimonthly (May–June) differences of (a) 850-hPa winds (m s^{-1}), (b) 500-hPa streamfunction (10^6 m^2 s^{-1}) and (c) 200-hPa winds (m s^{-1}) for the epoch 1958–1976. (d)–(f) as in (a)–(c), but for the epoch 1980–1998. Shading denotes regions of the t-test significance at the 95% confidence level. For wind fields, shading indicates regions where at least one of the wind components passes the 95% significance level.

parallel dashed lines for the period 1958–1976 represent 0.6σ, while those for the period 1980–1998 denote 0.8σ, in which σ is the standard deviation during each epoch. In fact, the actual SCMR anomalies denoted by the parallel dashed lines in 1958–1976 are identical with those in 1980–1998, and the absolute value of these anomalies equals 2.6 mm day^{-1}. Therefore, we use the identical thresholds for the two epochs to categorize a wet (dry) SCMR year as the one with its anomaly greater (less) than 2.6 (−2.6) mm day^{-1}. In addition to considering the requirement of the statistical significance test for sample size, the use of the thresholds also assures that the departures of the selected anomalous SCMR years exceed half of one standard deviation. Thus, in 1958–1976, the wet SCMR category includes 1959, 1966, 1970, 1972, 1973 and 1975, while the dry category includes 1958, 1961, 1963 and 1967. During 1980–1998, the wet SCMR category consists of 1982, 1989, 1992, 1993, 1997 and 1998, while the dry category consists of 1985, 1988, 1990, 1994 and 1995. Since the anomalies associated with the wet and dry SCMR generally tend to have opposite polarities, the composite wet-minus-dry differences represent simply anomalies related to the wet SCMR. The reverse is true for the dry SCMR, and thus the comparison is based on the wet SCMR flow patterns.

Figure 6 displays the composite wet-minus-dry differences of 850-hPa winds, 500-hPa streamfunction and 200-hPa winds during early summer (May–June) for the epochs 1958–1976 and 1980–1998. In 1958–1976, a significantly anomalous anticyclone is present over the South China Sea (SCS) and western Pacific such that South China is under the influence of anomalous southwesterlies (Figure 6(a)), favouring a wet SCMR due to much more moisture transport by the anomalous southwesterlies (Lu, 2001; Mao and Wu, 2006). Anomalous cyclonic and anticyclonic circulations are observed alternately to the north along 35°N and 50°N, respectively. Such a meridional juxtaposition of anomalous anticyclonic, cyclonic and anticyclonic circulations also exists

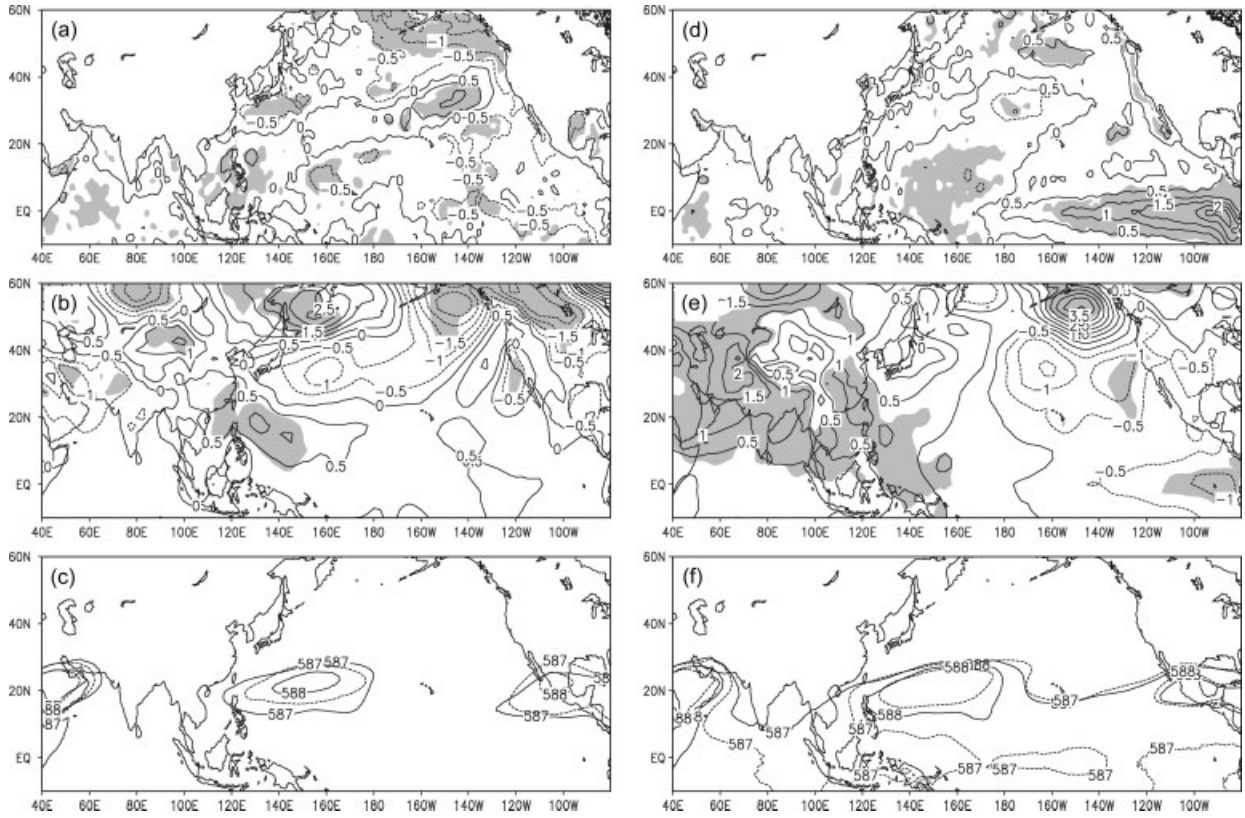

Figure 7. Composite wet-minus-dry bimonthly (May–June) differences of (a) SST (K) and (b) SLP (hPa) for the epoch 1958–1976. (c) Composite 500-hPa geopotential height indicated by 588 and 587 dam for wet (solid curves) and dry (dashed curves) SCMR years during 1958–1976. (d)–(f) as in (a)–(c), but for the epoch 1980–1998. Shading denotes regions of the t-test significance at the 95% confidence level.

clearly in the middle troposphere (Figure 6(b)), exhibiting a distinct wave train emanating from the tropical western Pacific (Nitta, 1987; Kawamura *et al*., 1996). A large anomalous anticyclone exists at 200 hPa just over the counterpart at 850 hPa, with significant westerly anomalies from western China to northern Pacific (Figure 6(c)), forming an anomalous upper-level divergent condition along the coast of South China. The meridional wave train patterns on the three isobaric surfaces are similar to spatial structures associated with the strong western North Pacific summer monsoon shown by Wang *et al*. (2001) except for opposite signs of the anomalous circulations.

In contrast, during 1980–1998, a relatively weak anomalous anticyclone also exists over the SCS, which can be identified by significant easterlies over the southern half of the SCS and southwesterlies over South China (Figure 6(d)). Since local rainfall amount depends largely on moisture convergence, and the moisture is mainly transported by the low-level southwesterly jet at the northwestern edge of the western North Pacific subtropical high (WNPSH) over East Asia (Lu, 2001), the weak anomalous southwesterlies would supply less moisture towards South China. Thus, this weak anomalous anticyclone may be responsible for the reduction of the SCMR standard deviation as compared with the period 1958–1976. In addition, there is no significant meridional wave-like coupling from tropics to middle-high latitudes along the coast of western North Pacific. Instead, pronounced anomalous easterlies are found from the SCS to the Arabian Sea, which might be associated with the breakdown of the negative relationship between Indian summer monsoon and ENSO (Kumar *et al*., 1999). Some of these features in the lower troposphere are also consistent with those given by Chang *et al*. (2000b), who used the reanalysis data from the National Centers for Environmental Prediction–National Center for Atmospheric Research and showed that the anomalous anticyclone in the northern SCS is clearly visible from May to July in 1951–1977, but in 1978–1996 it is considerably weaker in May and June and disappears in July. In correspondence with the low-level easterly anomalies, an anomalous anticyclone exists over the southern part of Asian continent and northern Indian Ocean in the middle troposphere, with an anomalous cyclone centred over northwestern China to the north. Significant westerly anomalies in the upper troposphere prevail over the Indian Ocean (Figure 6(f)), which are opposite with the lower tropospheric easterly anomalies, indicating a baroclinic structure in the Tropics.

The circulation structures responsible for wet and dry SCMR anomalies may be related to external forcing such as SST anomalies. In 1958–1976, negative SST anomalies are found in the equatorial eastern Pacific but not very significant, with positive SST anomalies in the equatorial western Pacific and midlatitude North Pacific (Figure 7(a)), exhibiting a SST anomaly distribution slightly similar to that of a La Niña event. It should be

noted that not all anomalous SCMR years are associated with ENSO events. On the other hand, most ENSO events in 1958–1976 generally reach their mature phases in early winter, and the magnitudes of SST anomalies decrease evidently during spring (Wang, 1995; Webster *et al*., 1998). Therefore, the entire distribution shows a La Niña-like pattern with SST anomalies being not very significant. Corresponding to the anomalous low-level winds shown in Figure 6(a), the SLP anomalies (Figure 7(a)) also manifests as a meridional wave train pattern over the western North Pacific, with significant positive anomalies over the Philippine Sea and with negative and positive anomalies to the north, respectively (Figure 7(b)). Note that in Figure 6(a), the significant anomalous easterlies around Philippine Sea in the lower troposphere may be related to the positive SST anomalies in the equatorial western Pacific due to convective activities (Nitta, 1987), though the anomaly magnitudes are not large.

Many previous studies (e.g. Tao and Chen, 1987; Mao and Wu, 2006) have shown that the location of the heavy rain belt over eastern China is closely related to that of the 500-hPa subtropical high over western North Pacific. Climatologically, the SCMR occurrences coincide with the ridgeline of the 500-hPa subtropical high locating around 18°N; when the ridgeline reaches 20°N, the Yangtze Meiyu starts. These imply that the interannual variations of the 500-hPa subtropical high in the location and strength could lead to the interannual SCMR variations. As suggested by Chang *et al*. (2000a), the relationships between East Asian summer monsoon and eastern Pacific SST anomalies are mostly due to the variations of the WNPSH ridge on both interannual and interdecadal timescales. The differences of subtropical highs in strength and location indicated by the 587- and 588-dam contours over the western North Pacific illustrate that in 1958–1976, the subtropical high related to the wet SCMR covers a larger extent and extends more westward than that of the dry SCMR (Figure 7(c)).

In 1980–1998, however, positive SST anomalies are very significant in the equatorial eastern Pacific, accompanied by negative SST anomalies in the western Pacific (Figure 7(d)), forming a SST anomaly distribution similar to that of an El Niño event. Note that the evolutions of some ENSO events during this epoch exhibit some different characteristics from those during 1958–1976 (Wang, 1995; Webster *et al*., 1998). For example, the 1986/87 El Niño event started warming in the equatorial central Pacific rather than in the eastern Pacific, and it matured in boreal summer rather than in winter. Thus, Figure 7(d) shows a distinct El Niño-like SST anomaly pattern. These imply that a wet SCMR is more likely related to an El Niño event. Compared with Figure 7(a), such nearly opposite SST anomaly patterns between the two epochs further demonstrate that the possible impact of ENSO events on the interannual variability of SCMR has undergone an interdecadal change.

Looking at the SLP responses (Figure 7(e)), negative SLP anomalies correspond to the positive SST anomalies in the equatorial eastern Pacific, while significant positive anomalies appear over the Philippine Sea and its west regions. The anomalous high pressure over the Philippine Sea along with the anomalous low-level anticyclone possibly result from a Rossby-wave response to suppressed convective heating (Nitta, 1987; Wang *et al*., 2000), which could be induced by both *in situ* ocean surface cooling and subsidence forced remotely by the equatorial central and eastern Pacific warming (Figure 7(d)). As suggested by Wang *et al*. (2000), the positive feedback resulting from the thermodynamic coupling of the atmospheric Rossby waves and the oceanic mixed layer in the presence of strong remote forcing might also contribute to the generation and maintenance of the anomalous anticyclone over the Philippine Sea. Although two 588-dam contours are clearly present over the western North Pacific, and the 587-dam contours both extend westward into the SCS or further to the west (Figure 7(f)), the differences between the wet and dry composites in 1980–1998 are not very large as compared to the period 1958–1976. Note that the discernable 587-dam contours appearing over the northern Indian Ocean represent a weak monsoon trough in 1980–1998, reflecting the role of positive PDO background in which positive circulation anomalies prevail in the Tropics.

4.2. Precursory signals

Chan and Shi (1999) found that some planetary circulation indices such as the 500-hPa zonal wind index over Eurasia in the preceding winter months correlated with the subsequent SCMR, and tried to use the technique of projection pursuit regression to derive prediction equations. To examine antecedent signals relating to the interannual SCMR variability, Figure 8 presents the composite wet-minus-dry differences of 850-hPa winds, 500-hPa streamfunction and 200-hPa winds in the preceding winter (January–February) for the epochs 1958–1976 and 1980–1998. In 1958–1976, striking southerly anomalies prevail from the SCS to the Lake Baikal in the lower troposphere (Figure 8(a)), which suggests that a wet SCMR is preceded by a weak winter monsoon. Associated with these anomalous southerlies is a significant anomalous cyclone locating around the Ural Mountain. A similar cyclonic anomaly exists in both the middle and upper troposphere (Figure 8(b) and (c)), and it is just over the anomalous cyclone in the lower troposphere, exhibiting an evident barotropic structure. The cyclonic anomaly in the middle and upper troposphere over the Ural Mountain implies a weak high-pressure ridge over Eurasian continent, which suggests a weak large-scale descending atmospheric motion and a weak Siberian high. Noteworthy are the anomalous upper tropospheric easterlies prevailing over the East Asian area in the middle latitudes (Figure 8(c)). As noted by Zhang *et al*. (1996), the anomalous upper tropospheric easterlies reduce the intensity of the climatological westerly jet stream in the

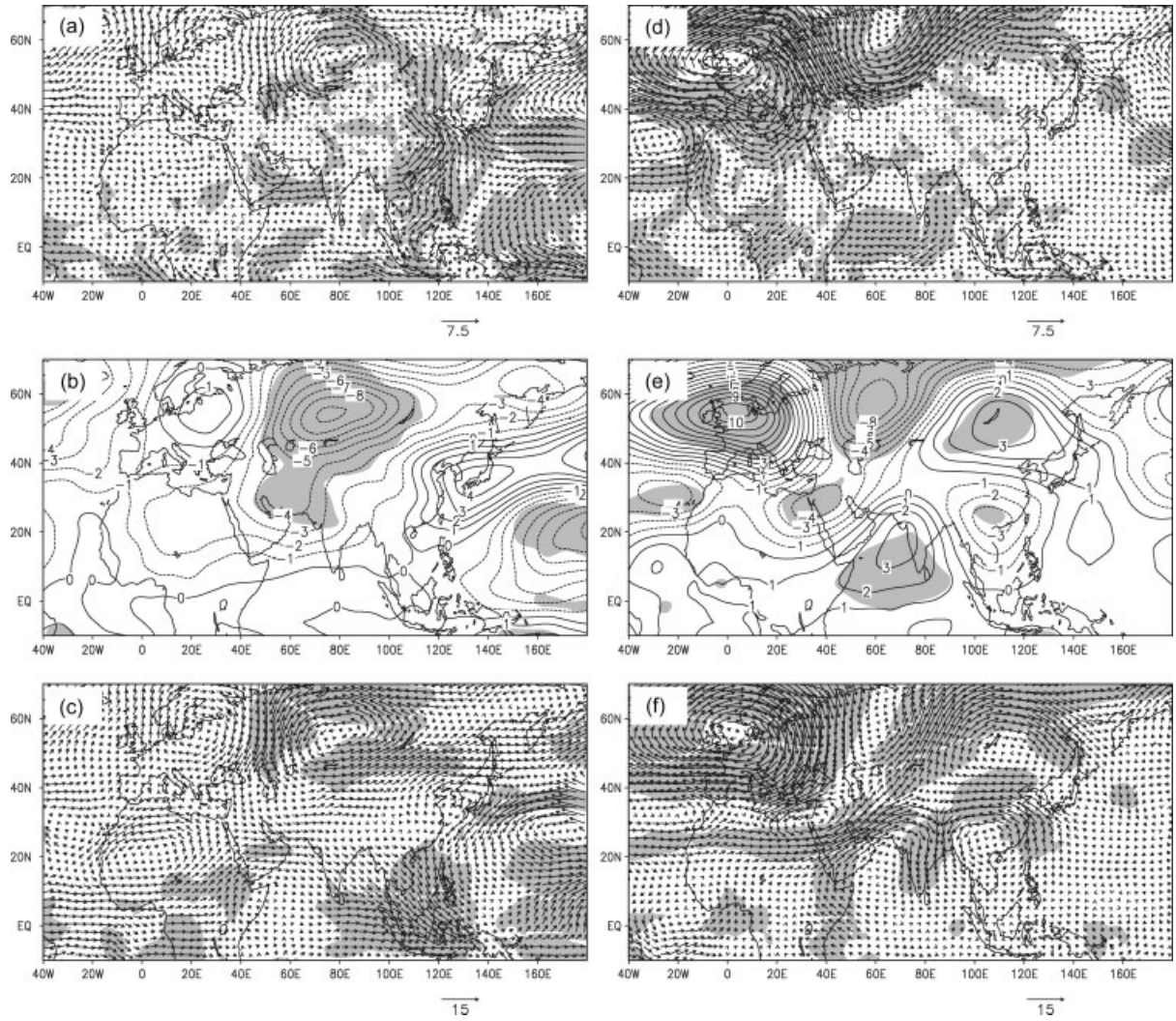

Figure 8. Composite wet-minus-dry bimonthly (January–February) differences of (a) 850-hPa winds (m s^{-1}), (b) 500-hPa streamfunction (10^6 m^2 s^{-1}) and (c) 200-hPa winds (m s^{-1}) for the epoch 1958–1976. (d)–(f) as in (a)–(c), but for the epoch 1980–1998. Shading denotes regions of the *t*-test significance at the 95% confidence level. For wind fields, shading indicates regions where at least one of the wind components passes the 95% significance level.

middle latitudes, and the weakening of westerly jet stream over East Asia is accompanied by a weak winter monsoon (Chang and Lau, 1982). Also noted are significant circulation anomalies in the troposphere over the tropical western Pacific, with easterly anomalies in the lower troposphere and westerly anomalies in the upper troposphere (Figure 8(a) and (c)), which may reflect atmospheric responses to the in-phase relation between PDO and ENSO, because such circulation anomalies exhibit some basic features during a cold ENSO phase or La Niña episode.

In contrast, in 1980–1998 a significantly coherent long wave train teleconnection, which exists in the lower, middle and upper troposphere and exhibits a dominant barotropic structure, emanates from the Atlantic to northeastern Asia (Figure 8(d)–(f)), suggesting that this wave train is possibly induced by the Atlantic Ocean SST anomalies. The wave train includes a cyclone over the tropical Atlantic Ocean, an anticyclone over the northern Europe, a cyclone over the Ural Mountain, and an anticyclone over the northeastern Asia, with the two middle cells being most significant. The anomalous anticyclone over northern Europe implies that in the troposphere, the actual high-pressure ridge along the west coast of Eurasian continent extends more northward in such a way that the colder air from the Arctic Ocean mainly moves towards East Asia. An anomalous anticyclone thus appears over northeastern Asia at the same time. Another precursory signal in the middle and upper troposphere is a prominent dipole anomaly pattern characterized by an anomalous anticyclone over South Asia and an anomalous cyclone over South China. This short wave pattern is out of phase with the long wave train in the middle-high latitudes, suggesting an interaction between tropical and extratropical waves (Chang *et al*., 2001). However, no significant anomalous signals are found over the western Pacific, indicating that the circulation anomalies associated with ENSO events are suppressed, which may result from the opposite effects of ENSO and PDO.

A comparison between the two panels in Figure 8 indicates that in 1958–1976 anomalous SCMR is preceded by a monopole circulation anomaly over the Ural Mountain in the preceding winter, while in 1980–1998 anomalous SCMR is preceded by a remarkable wave train teleconnection pattern in the middle-high latitudes, with alternately cyclonic and anticyclonic anomalies over the Atlantic Ocean, northern Europe, Ural Mountain and northeastern Asia. Note that in both epochs the circulation anomalies occurring around the Ural Mountain are statistically significant, suggesting that the circulation anomaly over this region is an important precursory signal to improve the seasonal forecasting of SCMR.

To further examine the remote influence of the middle-high latitude teleconnection wave train on the interannual SCMR variability, we have calculated the correlations of SCMR index with 500-hPa geopotential height field. Significant correlation distributions show quite similar features as in Figure 8. The scatter diagrams (Figure 9) of SCMR index with area-averaged 500-hPa geopotential height anomalies over the northern Europe (50°–60°N, 10°W–15°E) and the Ural Mountain (50°–65°N, 55°–65°E) in the preceding winter (January–February) for the period 1980–1998 show correlations of 0.71 and −0.62, respectively, both of which are statistically significant at the 99% confidence level. This supports the potential predictability of SCMR based on the planetary circulation indices as suggested by Chan and Shi (1999), but the circulation index to be used as predictors is actually different from epoch to epoch. As stated above, during 1958–1976 anomalous SCMR is linked with weak wave train pattern, with only significant correlation between SCMR index and area-averaged height over the Ural Mountain (55°–65°N, 65°–75°E) being −0.53 (Figure 10).

Actually, some previous studies have shown that the interannual variability of East Asian summer monsoon may be linked with the preceding winter monsoon (e.g. Ji *et al*., 1997; Chen *et al*., 2000), and this connection is mainly through the Pacific SST anomalies as well as the land-surface anomalies in temperature and moisture, because the atmospheric memory is shorter than that of the ocean and land (Wang *et al*., 2000). Since the winter atmospheric anomalies cannot persist for several months without any external forcing, the dynamical connection between the winter atmospheric teleconnection in middle-high latitudes especially for the anomalies over the Ural Mountain and anomalous SCMR is difficult to explain by atmospheric processes themselves. As shown by Chen *et al*. (2000), the WNPSH in the summer tends to shift northward after a strong East Asian winter monsoon but southward after a weak one. In addition, SST anomalies in the SCS and the western North Pacific may be a possible 'memory as well'. Wang *et al*. (2000) also suggested that the Asian winter monsoon variability can have considerable impacts on the formation and maintenance of the Pacific–East Asian teleconnection

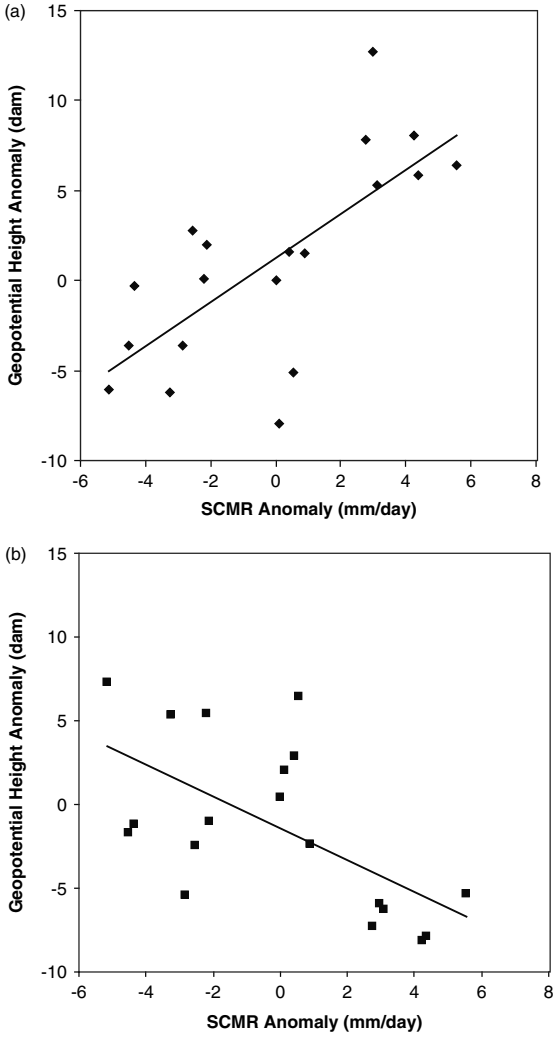

Figure 9. Scatter diagrams of (a) SCMR and area-averaged 500-hPa geopotential height anomalies over 50°–60°N, 10°W–15°E and (b) SCMR and area-averaged 500-hPa geopotential height anomalies over 45°–55°N, 55°–65°E in the preceding winter (January–February) for the period 1980–1998. Solid line is the best-fit linear regression line.

through the interaction between extratropical and tropical circulations.

These hypotheses could be supported by the modelling results of Ji *et al*. (1997), who used the long-term integrations of Max-Plank Institute ECHHM3 model to reveal the response of the Asian winter monsoon to the Pacific SST anomalies and its impact on the following summer monsoon. The apparent effect of a strong winter monsoon is found to enhance the convection over the tropical western Pacific. This effect, on the one hand, leads to a strengthening of southeast trades to the east and enhanced westerly flow to the west, thus favourable to maintain a specific SST anomaly pattern. On the other hand, the thermal forcing associated with SST anomaly acts to strengthen the extratropical flow pattern which is, in turn, conducive to stronger monsoon activity. Both the air–sea and tropical–extratropical interactions were suggested to play important roles in the development of western North Pacific cooling and wind anomalies

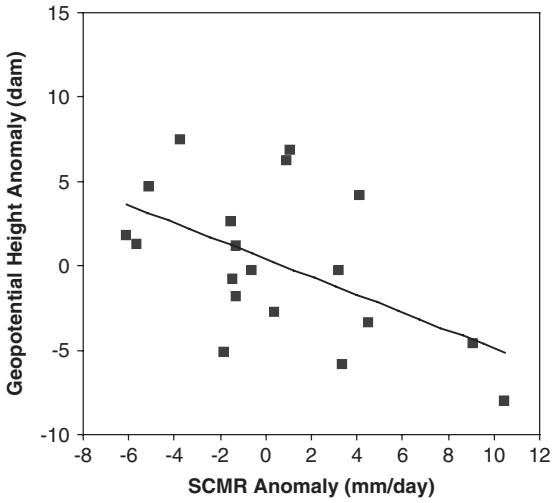

Figure 10. Scatter diagrams of SCMR and area-averaged 500-hPa geopotential height anomalies over 55°–65°N, 65°–75°E in the preceding winter (January–February) for the period 1958–1976. Solid line is the best-fit linear regression line.

with intermittent outburst of winter cold surge as links. Ji *et al.* (1997) thus pointed out that the connection between the strength of the Asian winter monsoon and the summer precipitation over China is mainly through SST anomalies but snow cover over Asia is a contributing factor as well.

As shown in Figure 8(a), during the epoch 1958–1976, the weak Asian winter monsoon could conceivably not cause too much cooling over the SCS and western Philippine Sea in winter and spring, and thus it could warm up earlier as seen in Figure 7(a), providing more moisture towards South China for convection in the early summer. On the other hand, the negative circulation anomaly over the Ural Mountain indicates the surface Siberian high pressure weaker than normal, implying inactive cold surges over the Asian continent, and leading to less cooling over land (less snow cover). These indicate that the East Asian continent could get heated up faster, favouring the formation of continental low pressure and the establishment of southwesterlies along the coast of South China in early summer, and thereby a wet SCMR.

However, for the epoch 1980–1998 the wet SCMR follows a strong winter atmospheric teleconnection pattern as in Figure 8(d). The anticyclonic anomaly near the Lake Baikal at 500 hPa to the east of the Ural Mountain cyclonic anomaly suggests an enhanced high-pressure ridge, which could cause cold air to move more southeastward and lead to strong cooling in the western Pacific from winter to spring. The significant negative SST anomalies in the western Pacific east of the Philippine Sea in the early summer (Figure 7(d)) are due to such cooling and the long memory of SST anomalies. In turn, such negative SST anomalies induce an anomalous anticyclone as a Rossby-wave response to suppressed convective heating (Wang *et al.*, 2000), with the subsidence forced remotely by the equatorial eastern Pacific warming also contributing to the anomalous anticyclone formation. On the other hand, as stated above, the winter cyclonic anomaly over the Ural Mountain could lead to above-normal surface air temperature over the Asian continent from winter to early summer, forming a thermal contrast with the cold western Pacific, which might also contribute to the wet SCMR. Further investigations will be required to verify these hypotheses.

The above analyses show an indirect influence of the anomalous Asian winter monsoon on the interannual variability of SCMR via both air–land and air–sea interactive processes in which anomalous extratropical circulations force SST anomalies and land-surface temperature anomalies as well as ground wetness anomalies. So the wintertime anomalous circulation signals may not always persist in the spring season, because they would affect the land-surface condition of the Eurasian continent and sea-surface condition of the North Pacific (Ji *et al.*, 1997). In turn, the changed surface conditions could influence the subsequent circulations (Webster *et al.*, 1998). Actually, the corresponding composite wet-minus-dry differences of 850-hPa winds, 500-hPa streamfunction and 200-hPa winds in the preceding spring (March–April) for the epochs 1958–1976 and 1980–1998 (not shown) indeed exhibit some similar and dissimilar features as depicted in Figure 8. Apparent changes are noted to take place in the intensity and location of the flow patterns as well as associated statistical significance.

In 1958–1976, the anomalous southerlies over eastern China weaken in the lower troposphere so that an anomalous anticyclone appears over the western Pacific east of the Philippines, which is similar to the counterpart in early summer except for a more eastward position as compared with Figure 6(a). In fact, along the western coast of the North Pacific, the meridional juxtaposition of anomalous anticyclonic, cyclonic and anticyclonic circulations becomes very evident. At 500 hPa, northern China is under the influence of an anomalous cyclone. In the upper troposphere, the anomalous cyclone extends southeastward in comparison with Figure 6(c); significant westerly anomalies thus prevail over the Tibetan Plateau across southern Japan into the North Pacific. In 1980–1998, weak southwesterly anomalies in the lower troposphere occur over the northern SCS, while easterly anomalies still exist over the equatorial northern Indian Ocean. The corresponding anomalous anticyclonic circulation is present at 500 hPa over the northern Indian Ocean, with the upper tropospheric westerly anomalies occurring over the eastern Africa and Indian continents.

Therefore, the winter precursory signals in the troposphere associated with anomalous SCMR show some similarities and differences between the two epochs. In addition to the similar circulation anomalies occurring around the Ural Mountain, remarkable differences exist in terms of wave train teleconnections. An anomalous SCMR follows a weak wave train pattern during 1958–1976, while it follows a strong wave train pattern during 1980–1998. The precursor signals appear to

have a barotropic structure in the extratropics. Considering their robustness, these signals should be of great importance for the seasonal prediction of SCMR.

4.3. Relative contribution of ENSO

The above results show that the interannual variability of SCMR is modulated by decadal-scale fluctuations in the Pacific SST anomalies. On interannual timescale, however, ENSO is the dominant signal in the coupled atmosphere-ocean system. Figure 7 illustrates that wet SCMR seems to be related to negative SST anomalous in the equatorial eastern Pacific in 1958–1976 such as years 1970, 1973 and 1975, while in 1980–1998 wet SCMR appears to be associated with positive SST anomalies there such as years 1982, 1992 and 1997. But such an ENSO–SCMR relationship exhibits a seasonal dependency. The precursory ENSO signals in the preceding winter and spring are relatively weak. Indeed, no significant SST anomalies are found over the Niño regions in the tropical Pacific from the composite wet-minus-dry differences of SST anomalies in the preceding winter (January–February) for both epochs 1958–1976 and 1980–1998 (not shown), although the peak phases of most ENSO events tend to occur during the period from November to February. Apparent exceptions occur in 1982/83 and in 1986/87, with the eastern Pacific peak warming in spring and summer fairly different from the events during the period 1958–1976 (Wang, 1995; Webster *et al*., 1998). Note also that not all anomalous SCMR years are associated with ENSO events. Such imperfect relationship between ENSO and SCMR indicates an inherent limitation to their linkage, suggesting that ENSO may not be the only factor involved in producing the observed SCMR anomalies on interannual timescale, because the ENSO effect is modulated not only by PDO (Gershunov and Barnett, 1998; Diaz *et al*., 2001) but also by other causes such as Eurasia snow cover (e.g. Barnett *et al*., 1989). On the other hand, the ENSO impact on SCMR may be 'delayed' or 'indirect' (Chan and Zhou, 2005).

Some studies suggested that the Asian summer monsoon rainfall anomalies are related to the phases of an ENSO event (e.g. Wang *et al*., 2001; Wu and Wang, 2002). To examine the relationships between ENSO and SCMR anomalies further, several El Niño and La Niña events during each epoch are identified based on the Niño 3.4 index (Trenberth, 1997). Because most ENSO events generally extend across different calendar years and persist for two full years, a typical ENSO event can be generally considered to start in January of the year in which El Niño and La Niña conditions occur and end in December of next year. As mentioned above, the peak phases of most events tend to mature in boreal winter. During a cycle of an individual ENSO event, the first year belongs to the developing phase while the second year belongs to the decaying phase. Table I lists the SCMR anomalies associated with these events. In 1958–1976, wet or dry SCMR preferences are not found to be dominant in both the developing and decaying phases of an El Niño event. But the developing phase of a La Nina event appears to favour a wet SCMR with normal SCMR preference in its decaying phase. However, in 1980–1998, both the developing and decaying phases of an El Niño event favour a wet or normal SCMR. Only two dry SCMR years are associated with El Niño events. No preference of the anomalous SCMR is found under La Niña situations. These results suggest that in epoch 1980–1998, the wet SCMR may be more likely associated with an El Niño event, while in 1958–1976 the wet SCMR is more likely related to a La Niña event. It should be mentioned that these statistical results are merely qualitative analyses, because the sample size is not large enough.

Table I. SCMR anomalies during different ENSO phases for two epochs[a].

Epoch	1958–1976	1980–1998
El Niño	1957 (+)–1958 (−)	1982 (+)–1983 (0)
Ratio of +/−	1963 (−)–1964 (0)	1986 (0)–1987 (0)
	1965 (0)–1966 (+)	1991 (0)–1992 (+)
	1968 (0)–1969 (0)	1992 (+)–1993 (+)
	1972 (+)–1973 (+)	1994 (−)–1995 (−)
	2/1 2/1	1997 (+)–1998 (+)
La Niña	1964 (0)–1965 (0)	3/1 3/1
Ratio of +/−	1967 (−)–1968 (0)	1984 (0)–1985 (−)
	1970 (+)–1971 (0)	1988 (−)–1989 (+)
	1973 (+)–1974 (0)	1995 (−)–1996 (0)
	1975 (+)–1976 (0)	1998 (+)–1999 (−)
	3/1 0/0	1/2 1/2

[a] El Niño or La Niña years are based on the Niño3.4 index (Trenberth, 1997). Here, +, − and 0 in parentheses indicate the SCMR anomaly magnitude, respectively, corresponding to the wet, dry and normal SCMR shown in Figure 5.

As pointed out by Webster *et al*. (1998), despite the importance of the ENSO phenomenon in climate variability on seasonal-to-interannual timescales, ENSO does not explain all of the variance. Instead, the midlatitude wave train patterns are more evident during winter months in the atmospheric circulation of the Northern Hemisphere, especially in the epoch 1980–1998 (Figure 8). These suggest that the internal variability of the atmosphere circulation should also be considered. After all, the impact of ENSO on rainfall has to be realized via the 'atmospheric bridge' mechanism (Lau, 1997). Chan and Zhou (2005) noted that the effects of ENSO and PDO on SCMR are through modifying the intensity of the subtropical high. Thus, the actual SCMR anomaly depends on anomalous circulation pattern determined by the interaction between internal atmospheric variability and external forcing.

5. Conclusion and discussion

The interannual variations of the early summer monsoon rainfall over South China (SCMR) are modulated by interdecadal fluctuations in association with Pacific Decadal Oscillation (PDO). Such interannual variations

relative to different PDO backgrounds are examined based on station rainfall data, the Hadley Centre's products, and the ERA-40 reanalysis data. The objective of this study is to investigate the atmospheric circulation patterns responsible for interannual SCMR variations, thereby understanding the interdecadal modulations of SCMR variations and the causes for the extreme wet and dry SCMR.

Based on the evolution of PDO index, two epochs are classified with the dominantly negative PDO phase during 1958–1976 and positive phase during 1980–1998. The variance of interannual SCMR variations is larger during 1958–1976 than during 1980–1998, which reflects an interdecadal change of SCMR. The interdecadal SST anomaly differences between these two epochs show that during 1958–1976, the entire pattern in the Pacific and Indian Oceans displays some features similar to a La Niña event, and persists unusually from the preceding winter months to early summer, while during 1980–1998, unusually persistent SST anomalies of an El Niño-like pattern are prominent, implying that El Niño events predominate over La Niña events during this epoch. Composite SLP anomalies demonstrate that during the negative PDO phase, major atmospheric response is roughly a dipole anomaly pattern characterized by negative SLP anomalies over the western and central Pacific from 0° to 20°N and positive anomalies over the eastern Aleutian Basin. Such positive anomalies over the Aleutian Basin possibly represent a typical response of the negative PDO–La Niña combination. During the positive PDO phase, persistent positive pressure anomalies exist over tropical western and central Pacific, with negative anomalies over the Aleutian Basin.

The interdecadal differences in the middle and upper troposphere show that during the negative PDO phase, a pair of zonally stretched anomalous anticyclonic circulations is present over midlatitudes, one covering the Eurasia continent and the other covering the midlatitude North Pacific, while anomalous cyclonic circulation prevails over the Tropics. Positive height anomalies centred over northwestern China and North Pacific are accompanied by negative height anomalies to the south, in a band covering most of the Tropics south of 20°N. The opposite flow patterns occur during 1980–1998, with anomalous cyclonic circulations prevailing over the midlatitudes and anomalous anticyclonic circulations in the Tropics. Thus, the interannual variation of SCMR over recent decades is inevitably influenced by such interdecadal circulation anomalies in midlatitudes and tropics.

The dominant atmospheric teleconnection patterns associated with extreme interannual variations of SCMR are remarkably different from the two epochs. In 1958–1976, a significantly anomalous anticyclone is present over the SCS and western Pacific so that South China is under the influence of anomalous southwesterlies, favouring a wet SCMR due to much more moisture transport by the anomalous southwesterlies. Anomalous cyclonic and anticyclonic circulations are alternately observed to the north along 35°N and 50°N, respectively. Such a meridional juxtaposition of anomalous anticyclonic, cyclonic and anticyclonic circulations also exists clearly in the midtroposphere. There is a large anomalous anticyclone present at 200 hPa, with significant westerly anomalies extending from western China to northern Pacific. The opposite flow pattern is for an anomalous dry SCMR. In contrast, in 1980–1998 although a relatively weak anomalous anticyclone also exists over the SCS for a wet SCMR, which may to some extent be responsible for the reduced SCMR standard deviation due to less moisture supply, there is no significant meridional wave-like coupling from tropics to middle-high latitudes along the coast of western North Pacific. Instead, pronounced anomalous easterlies blow from the SCS to the Arabian Sea.

The spatial circulation structures responsible for wet and dry SCMR anomalies may be related to Pacific SST anomalies. In 1958–1976, negative SST anomalies appear in the equatorial eastern Pacific but not very significant, with positive SST anomalies in the midlatitude North Pacific, implying that a wet SCMR might be associated with a La Niña-like event. In 1980–1998, however, positive SST anomalies are very pronounced, accompanied by negative SST anomalies in the western Pacific, indicating that the wet SCMR is more likely related to El Niño-like event. The SLP responses show that in 1958–1976, significant positive SLP anomalies exist over the Philippine Sea, with negative and positive anomalies to the north respectively, which corresponds to the lower tropospheric anomalous wind pattern. Significant positive SLP anomalies cover southern half of Asia including western Pacific in 1980–1998. The interannual variations of SCMR are closely related to those in the location and strength of the 500-hPa subtropical high. In 1958–1976, the subtropical high of the wet SCMR covers a larger extent and extends more westward than that of the dry SCMR. In 1980–1998, small differences exist in subtropical high between the wet and dry years, with weak monsoon trough over the northern Indian Ocean.

Strong precursor signals relating to an anomalous SCMR are found in the preceding winter. Composite results show that in 1958–1976, striking 850-hPa southerly anomalies prevail from the SCS to the Lake Baikal, suggesting that a wet (dry) SCMR usually follows a weak (strong) winter monsoon. Associated with these anomalous southerlies is a significant anomalous cyclone locating around the Ural Mountain. Similar patterns with a barotropic structure also exist in middle and upper troposphere. The anomalous cyclone indicates a weak high-pressure ridge over Eurasia continent, and an anomalous SCMR is thus preceded by a monopole circulation anomaly over the Ural Mountain in the preceding winter. In contrast, in 1980–1998 an anomalous wet (dry) SCMR follows a coherent long wave train teleconnection pattern in winter. Such a wave train emanates from the Atlantic to the northeastern Asia and exists in the lower, middle and upper troposphere with a dominant barotropic structure. Associated with the wave train are

the most significant 500-hPa geopotential height anomalies over northern Europe and Ural Mountain, implying that the height anomalies over these two areas are indicative of an anomalous SCMR. Another precursory signal in the middle and upper troposphere is a prominent dipole anomaly pattern characterized by an anomalous anticyclone (cyclone) over South Asia and an anomalous cyclone (anticyclone) over South China. This short wave pattern is out of phase with the long wave train in the middle-high latitudes, suggesting an interaction between tropical and extratropical waves. In both epochs, the circulation anomalies occurring around the Ural Mountain are significant, showing a highly negative correlation with anomalous SCMR. These suggest that the circulation anomaly over this region is an important precursory signal and could be useful for seasonal forecasting of SCMR.

Although ENSO is the dominant signal on interannual timescale, it may not be the only factor involved in producing the observed SCMR anomalies due to the modulation of PDO and other causes. The different precursory signals in two different epochs have been found in wintertime atmospheric circulation, but the physical mechanisms for the anomalous circulation subsequently affecting early summer circulation through air–land and air–sea interactions need to be further examined. As suggested by Wang *et al*. (2000) and Wu and Wang (2002), the relationship between the East Asian monsoon and ENSO is very complex. How external forcings induce the tropical and extratropical atmosphere to produce such different dominant patterns in the two epochs also deserves further study.

Acknowledgements

ECMWF ERA-40 data used in this study have been obtained from the ECMWF data server. SST and SLP data are obtained from http://hadobs.metoffice.com/. This research was supported by Innovation Project of Chinese Academy of Sciences (Grant KZCX2-YW-Q11-04), National Basic Research program of China (Grant 2006CB403603), and Natural Science Foundation of China (Grant 40975052).

References

Allan R, Ansell T. 2006. A new globally-complete historical gridded mean sea level pressure data set (HadSLP2): 1850–2004. *Journal of Climate* **19**: 5816–5842.

Barnett TP, Dumenil L, Schlese U, Roceckner E, Latif M. 1989. The effect of Eurasian snow cover on regional and global climate variations. *Journal of the Atmospheric Sciences* **46**: 661–685.

Barnett TP, Pierce DW, Latif M, Dommenget D, Sarvanan R. 1999. Interdecadal interactions between the tropics and midlatitudes in the Pacific basin. *Geophysical Research Letters* **26**: 615–618.

Chan JCL, Shi J. 1999. Prediction of the summer monsoon rainfall over South China. *International Journal of Climatology* **19**: 1255–1265.

Chan JCL, Zhou W. 2005. PDO, ENSO and the early summer monsoon rainfall over South China. *Geophysical Research Letters* **32**: L08810, DOI:10.1029/2004GL022015.

Chang CP, Lau KM. 1982. Short-term planetary-scale interactions over the Tropics and midlatitudes during northern winter. Part I: Contrasts between active and inactive periods. *Monthly Weather Review* **110**: 933–946.

Chang CP, Zhang Y, Li T. 2000a. Interannual and interdecadal variations of the East Asian summer monsoon and tropical Pacific SSTs. Part I: Roles of the subtropical ridge. *Journal of Climate* **13**: 4310–4325.

Chang CP, Zhang Y, Li T. 2000b. Interannual and interdecadal variations of the East Asian summer monsoon and tropical Pacific SSTs. Part II: Meridional structure of the monsoon. *Journal of Climate* **13**: 4326–4340.

Chang CP, Harr P, Ju J. 2001. Possible roles of Atlantic circulations on the weakening Indian monsoon rainfall–ENSO relationship. *Journal of Climate* **14**: 2376–2380.

Chen W, Graf HF, Huang R. 2000. The interannual variability of East Asian winter monsoon and its relation to the summer monsoon. *Advances in Atmospheric Sciences* **17**: 48–60.

Diaz HF, Hoerling MP, Eischeid JK. 2001. ENSO variability, teleconnections and climate change. *International Journal of Climatology* **21**: 1845–1862.

Ding Y. 1994. *Monsoons over China*. Kluwer Academic Publisher: London.

Ding Y. 2007. The variability of the Asian summer monsoon. *Journal of the Meteorological Society of Japan* **85B**: 21–54.

Gershunov A, Barnett TP. 1998. Interdecadal modulation of ENSO teleconnections. *Bulletin of the American Meteorological Society* **79**: 2715–2725.

Graham NE. 1994. Decadal-scale climate variability in the 1970s and 1980s: Observations and model results. *Climate Dynamics* **10**: 135–162.

Graham NE, Barnett T, Wilde R, Ponater M, Schubert S. 1994. On the roles of tropical and midlatitude SSTs in forcing interannual to interdecadal variability in the winter Northern Hemisphere circulation. *Journal of Climate* **7**: 1416–1441.

Hare SR, Mantua NJ. 2000. Empirical evidence for North Pacific regime shifts in 1977 and 1989. *Progress in Oceanography* **47**: 103–145.

Hurrell JW. 1995. Decadal trends in the North Atlantic oscillation: Regional temperatures and precipitation. *Science* **269**: 676–679.

Ji L, Sun S, Arpe K, Bengtsson L. 1997. Model study on the interannual variability of Asian winter monsoon and its influence. *Advances in Atmospheric Sciences* **14**: 1–22.

Kawamura R, Murakami T, Wang B. 1996. Tropical and mid-latitude 45-day perturbations over the western Pacific during the northern summer. *Journal of the Meteorological Society of Japan* **74**: 876–890.

Krishna R, Sugi M. 2003. Pacific decadal oscillation and variability of the Indian summer monsoon rainfall. *Climate Dynamics* **21**: 233–242.

Krishnamurthy V, Goswami BN. 2000. Indian monsoon–ENSO relationship on interdecadal timescale. *Journal of Climate* **13**: 579–595.

Kumar KK, Rajagopalan B, Cane MA. 1999. On the weakening relationship between the Indian monsoon and ENSO. *Science* **284**: 2156–2159.

Latif M, Barnett TP. 1996. Decadal climate variability over the North Pacific and North America: Dynamics and predictability. *Journal of Climate* **9**: 2407–2423.

Lau NC. 1997. Interactions between global SST anomalies and the midlatitude atmospheric circulation. *Bulletin of the American Meteorological Society* **78**: 21–33.

Lu R. 2001. Interannual variability of the summertime North Pacific subtropical high and its relation to atmospheric convection over the warm pool. *Journal of the Meteorological Society of Japan* **79**: 771–783.

Mantua NJ, Hare SR, Zhang Y, Wallace JM, Francis RC. 1997. A Pacific interdecadal climate oscillation with impacts on salmon production. *Bulletin of the American Meteorological Society* **78**: 1069–1079.

Mao J, Wu G. 2006. Intraseasonal variations of the Yangtze rainfall and its related atmospheric circulation features during the 1991 summer. *Climate Dynamics* **27**: 815–830.

McGowan JA, Cayan DR, Dorman LM. 1998. Climate–ocean variability and ecosystem response in the Northeast Pacific. *Science* **281**: 210–217.

Namias J, Yuan X, Cayan DR. 1988. Persistence of North Pacific sea surface temperature and atmospheric flow patterns. *Journal of Climate* **1**: 682–703.

Nitta T. 1987. Convective activities in the tropical western Pacific and their impact on the Northern Hemisphere summer circulation. *Journal of the Meteorological Society of Japan* **65**: 373–389.

Overland JE, Adams JM, Bond NA. 1999. Decadal variability of the Aleutian Low and its relation to high-latitude circulation. *Journal of Climate* **12**: 1542–1548.

Palmer TN, Anderson DLT. 1994. The prospects for seasonal forecasting – A review paper. *Quarterly Journal of the Royal Meteorological Society* **120**: 755–793.

Rayner NA, Parker DE, Horton EB, Folland CK, Alexander LV, Rowell P, Kent EC, Kaplan A. 2003. Global analyses of sea surface temperature, sea ice, and night marine air temperature since the late nineteenth century. *Journal of Geophysical Research* **108**: 4407, DOI:10.1029/2002JD002670.

Shukla J, Paolino DA. 1983. The Southern Oscillation and long range forecasting of the summer monsoon rainfall over India. *Monthly Weather Review* **111**: 1830–1837.

Tao SY, Chen LX. 1987. A review of recent research of the East Asian summer monsoon in China. In *Monsoon Meteorology*, Chang CP, Krishnamurti TN (eds). Oxford University Press: New York; 60–92.

Torrence C, Webster PJ. 1999. Interdecadal changes in the ENSO–monsoon system. *Journal of Climate* **12**: 2679–2690.

Trenberth KE. 1990. Recent observed interdecadal climate changes in the Northern Hemisphere. *Bulletin of the American Meteorological Society* **71**: 988–993.

Trenberth KE. 1997. The definition El Niño. *Bulletin of the American Meteorological Society* **78**: 2771–2777.

Wang B. 1995. Interdecadal changes in El Niño onset in the last four decades. *Journal of Climate* **8**: 267–285.

Wang B, Wu R, Fu X. 2000. Pacific–East Asian teleconnection: How does ENSO affect East Asian climate? *Journal of Climate* **13**: 1517–1536.

Wang B, Wu R, Lau KM. 2001. Interannual variability of the Asian summer monsoon: contrasts between the Indian and the western North Pacific–East Asian monsoons. *Journal of Climate* **14**: 4073–4090.

Webster PJ, Yang S. 1992. Monsoon and ENSO: Selectively interactive systems. *The Quarterly Journal of the Royal Meteorological Society* **118**: 877–926.

Webster PJ, Magaña VO, Palmer TN, Tomas RA, Yanai M, Yasunari T. 1998. Monsoons: processes, predictability, and the prospects for prediction. *Journal of Geophysical Research* **103**: 14451–14510.

Wu R, Wang B. 2002. A contrast of the East Asian summer monsoon–ENSO relationship between 1962–77 and 1978–93. *Journal of Climate* **15**: 3266–3279.

Zhang R, Sumi A, Kimoto M. 1996. Impact of El Niño on the East Asian monsoon: a diagnostic study of the '86/87 and '91/92 events. *Journal of the Meteorological Society of Japan* **74**: 49–62.

Zhang Y, Wallace JM, Battisti DS. 1997. ENSO-like interdecadal variability: 1900–93. *Journal of Climate* **10**: 1004–1020.

Zhou W, Li C, Chan JCL. 2006. The interdecadal variations of the summer monsoon rainfall over South China. *Meteorology and Atmospheric Physics* **93**: 165–175.

